

CHAPTER 3

The Hysteresis Effect in the **Recovery** of Damaged Aquatic Ecosystems: an Ecological Phenomenon with **Policy** Implications

Abstract

The individual species or functional components of an ecosystem can be expected to respond at different rates to the application and/or removal of pollutant stress. These rates are primarily dependent on the generation time (a function of body size and complexity) of the organism and its place in the **trophic** hierarchy (e.g. producer, grazer or carnivore). Even in the absence of population extinctions, a non-retraceable behavior (or hysteresis effect) is expected. Conceptually, the lower **trophic** levels will follow a series of nested hysteresis curves, while organisms at higher **trophic** levels, such as sports fish, will probably respond more erratically. To explore these issues, we develop an illustrative hysteresis **trophic-link** model (**HTLM**) that incorporates limited ecological reality but is simple enough to expand to an arbitrary number of functional groups. This model is compared to a conceptual model for biotic hysteresis for a system with three **trophic** levels. We show how hysteresis might influence population changes at higher **trophic** levels (e.g. fish) caused by pollution. These changes cannot be measured directly because large fish are difficult to sample with high precision.

Introduction

In most aquatic ecosystems damage occurs by two mechanisms. These are physical destruction (for example, lake edge filling) or chemical perturbation (notably, additions of **biostimulants** and **toxicants**). With the exception of

sediment **loading, most** pollutants regulated by the U.S. Environmental Protection Agency (EPA) cause damage by chemical perturbation of ecosystems.

It **is** often assumed that above the dose-response threshold, the change **in some** component of an aquatic ecosystem is linearly proportional to the amount of pollution, as for example in the **Dillon-Rigler** (1974), **Vollenweider** (1968), or **Vollenweider** and **Kerekes** (1980) phosphorus- (or nitrogen-) chlorophyll models of lake eutrophication. Studies on lake restoration have shown that non-linearity and time lags in the recovery of systems perturbed by pollution occur for at **least** some lakes (e.g. **Shagawa Lake**, **Maguey et al**, 1973; Lake Washington, **Edmondson**, 1972). The reasons for non-linearity have not been " well studied, but they appear to be partially due to the varying "turnover-times" of the physical, **abiotic**, and simple biotic components of a complete aquatic ecosystem (**Edmondson**, 1982; Home, unpublished). Further **step-function-type** responses and time lags may be introduced by "higher-order Interactions" that occur far from the site of the pollutant **action**. Examples of these interactions are species displacement such as **occured** for lake trout in the Great Lakes, or indirect competition from changes in species dominance (**Christie**, 1974). Given these complications, it is not surprising that the recovery of an ecosystem's more complex biotic levels, such as that of a damaged sports fishery, does not proceed either in a simple linear or virtually instantaneous manner upon removal of a pollutant load.

It is important to distinguish between the purely physiochemical and the biotic responses to removal of a pollutant from an aquatic ecosystem. All pollutants **will** decrease when the source is shut off and the internal pollutant load is diluted as new clean water flushes out the **system**. In many cases the pollutant load will be negligible in months or years--as is the case following the onset of phosphorus removal by new sewage-treatment plants (Goldman and Home, 1983, pp. 392-4). In any event the physiochemical

response **is** generally predictable from a knowledge of the pollutant? the hydraulic residence time **in** the system, the mean depth, and the characteristics of the bottom sediment.

.In contrast, the biotic response may be delayed or may occur **in** spurts. In extreme cases the **biota** may never return to their original states. The time path of ecosystem recovery **is** not predictable at present since the reasons for non-linearity are unclear. The response of the **biota** to a decrease in pollution may also **fail** to mirror the response of the system to the original increase in pollution, that is, the response may be **non-retraceable**. This paper attempts to provide a theoretical basis for a \square athematical description of the **biotic** restoration of damaged aquatic **ecosystems**. In particular the non-linear and **non-retracable** character of the process of recovery from pollution--defined here **as** the hysteresis effect--will be considered.

In the following sections we present the general methods and theoretical basis for the hysteresis **trophic-link** model (HTLM), describe in a theoretical way our concepts of 'ideal'^w and 'non-Ideal'^w **biotic** hysteresis show the specific form used for the HTLM and some initial results from the **modelling** effort, and discuss the merits and drawbacks of the HTLM approach in providing information useful **in** setting environmental policy.

Methods and Theoretical Basis

Time lag effects may have many sources, but it **is** most logical (in the sense of **Occam's** razor) to examine first the turnover time of the components of the ecosystem as a possible source. If a population **is** to recover quickly when the pollutant load is removed **it** must grow and breed quickly. Since the larger organisms depend on the smaller ones as food sources, populations of larger organisms cannot grow until populations of smaller organisms are in

place. The turnover time for **biota is** usually the generation time and can range from a few hours for simple bacteria and **algae** to decades for very large **fish** such as striped bass or sturgeon. Generation time **is** primarily a function of two variables: the sexuality of reproduction and the structural complexity of the adults. **Asexual** reproduction (vegetative or parthenogenetic reproduction) **is** typical of simple animals and plants growing under favorable conditions. Sexual reproduction **is** typical of more complex organisms or of simple ones growing under unfavorable conditions. Sexual reproduction uses more time than asexual reproduction, and confers few, **if** any, short-term benefits. In addition, complex organisms **must** spend time **in** building their large complex body structures. This involves several **moult**s, **a**long adolescence, and differing environmental requirements for adult and young, depending **on** the species involved. The organisms **in** the **trophic** levels usually present in aquatic ecosystems have the following typical characteristic sizes (length, **l**) and generation times (**gt**):

phytoplankton	l = 0.02 mm,	gt = 3 days
zooplankton	l = 1 mm ,	gt = 3 weeks
ichthyoplankton	l = 1 cm,	gt = 1 year
juvenile piscivorous and planktivorous adult fish	l = 5 cm ,	gt = 1 year
piscivorous fish	l = 20 cm,	gt = 3 years
large sports fish	l = 50 cm,	gt = 10 years.

The aquatic ecosystem we use in our model **is** simplified in the sense that side, across, and multiple-step (**omnivory**) food-chain **links** are omitted (Figure 1). Although this may seem like a major simplification when one considers the apparently highly cross-linked structure of some aquatic **food** webs (e.g. Figure 2), the dynamics of many food webs are **in** fact much **less** cross-linked, **in** terms of energy or food flow, than they appear to be. **This**



Figure 1. Schematic diagram of a **trophic-link** model. Here P describes the effect of the pollutant on each **trophic** level, and X is a measure of the biomass present for each functional class of organism (e.g. primary producers, filter-feeders, carnivores, etc.).

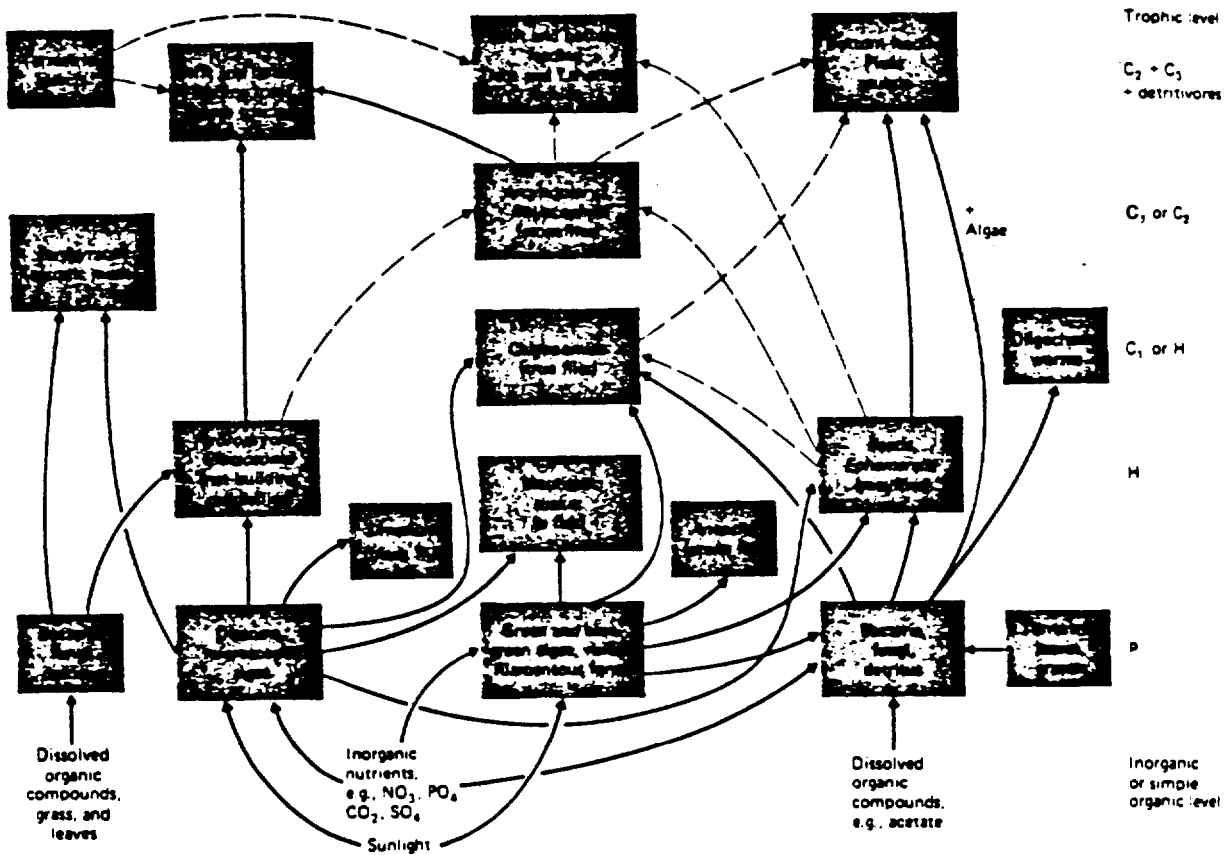


Figure 2. A qualitative food web for the Truckee River, California. **Solid** lines indicate measured pathways. Broken lines are **assumed** pathways derived from other **studies** of adjacent waters. Note that the omnivorous feeders (e.g. **dace**, **trout**, **sculpin**) use more than one **trophic** level. Most herbivores prefer microscopic diatoms to large **filamentous** green and blue-green algae. (Reproduced from Goldman and Home, 1983)

is illustrated by one of the few known quantitative examples of an aquatic food chain, that of the River Thames below Kennet mouth (Goldman and Home, 1983). Figure 3a shows the complete food web for the Thames system. As complicated as this looks, placing of the organisms in this web into functional groups results in the much more simplified structure shown in Figure 3b. Thus while the assumption of a linear food chain is certainly a simplification, it may not be a bad starting point for modelling some aquatic ecosystems.

In the linear food chain depicted in Figure 1, the rate of change of the phytoplankton population can be described by the equation

$$(1) \quad \frac{dX}{dt} = r_x(X)(1 - (X/K_x)) - B_{xy}XY - b_xX, \text{ where}$$

x = the population density of phytoplankton (e.g. chlorophyll a per cubic meter of water),

r_x = the maximal growth rate of the phytoplankton population,

K_x = a carrying capacity constant,

B_{xy} = a rate constant describing predation of zooplankton on phytoplankton,

Y = the population of zooplankton that feed on the phytoplankton (X), and

b_x = the rate of loss of phytoplankton due to washout and other linear, donor-controlled mechanisms.

In this system we assume that each organism eaten is killed and that no significant amount of prey is uneaten.

Analogous equations can be used to describe the rate of change of the higher trophic-level populations. For example:

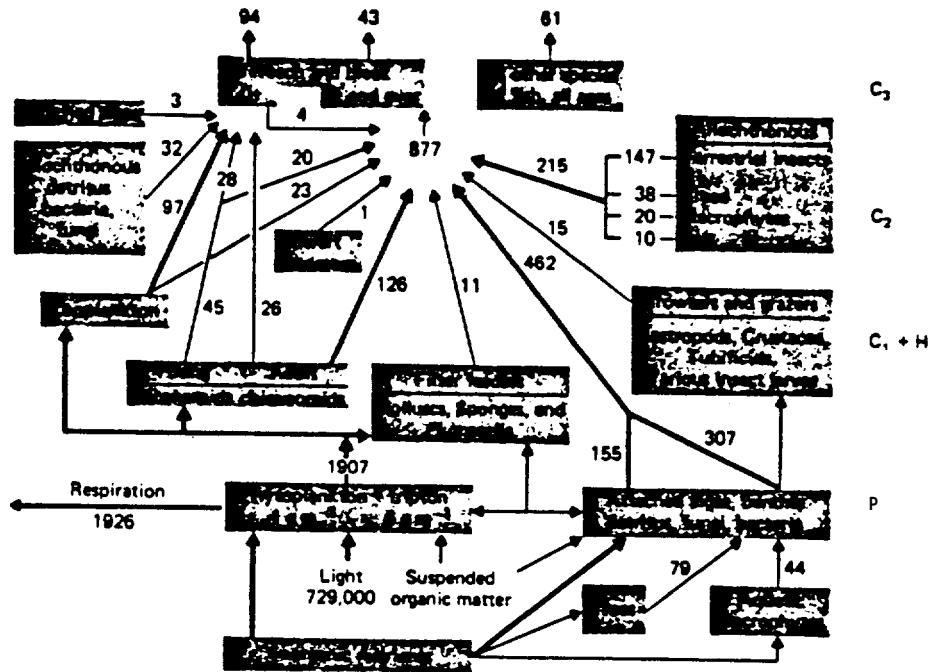


Figure 3a. This figure presents a dynamic food web for a natural system: an energy flowchart for the River Thames below Kennet mouth. In general, primary producers are shown at the bottom, invertebrate animals at the center, and fish at the top of the chart, but to avoid complex networks of arrows sources of attached algae, detritus, and allochthonous materials are shown in two places. Heavy arrows indicate the largest channels of energy flow. Note the twin flow of energy to fish from low-quality attached algae and high-quality animal food from terrestrial insects and adult chironomids. Energy input from dissolved organic matter was not measured directly. (Redrawn from Mann et al, 1972, reproduced from Goldman and Horne, 1983)

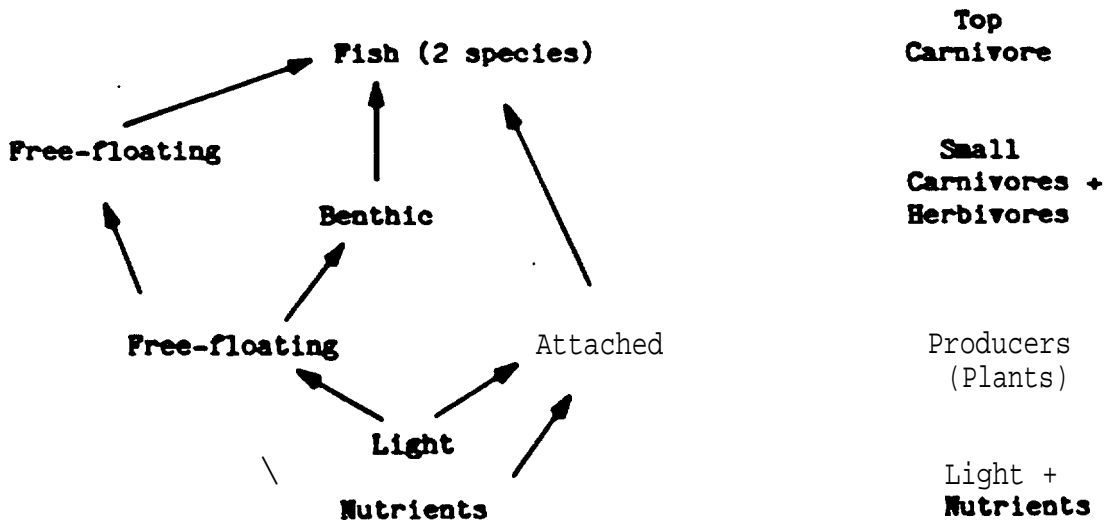


Figure 3b. The major energetic pathways from figure 3a. This diagram shows that modeling using single-link trophic models is possible if the organisms in the ecosystem are classified into functional rather than taxonomic groups.

$$(2) \quad \frac{dY}{dt} = E_{xy}B_{xy}XY - B_{yz}YZ - b_yY, \text{ where}$$

x , Y , and B_{xy} are as above,

E_{xy} = a factor describing the proportion of biomass consumed from trophic level x (phytoplankton) that is retained in trophic level y (zooplankton),

B_{yz} = a rate constant describing predation on zooplankton by ichthyoplankton (small fish that feed on zooplankton),

z = the population of ichthyoplankton, and

b_y = the loss rate of zooplankton due to washout, death, or other donor-related mechanisms.

This pair of equations can be expanded to an arbitrarily large set describing an arbitrarily long food chain.

Changes in pollution will affect some of the growth rates directly, but all populations will be affected as a result of trophic interactions. A straightforward example of such an interaction is the following. Suppose a pollutant acted so as to decrease the growth rate (r_x) of the phytoplankton in an aquatic ecosystem. This pollutant could be toxic to the phytoplankton or could be an inert pollutant like silt in a lake, that affects r_x by decreasing the light available for photosynthesis. In either case, a reduction in the phytoplankton growth rate reduces the phytoplankton population, which reduces the amount of food available to the zooplankton, which reduces the zooplankton population, which reduces the amount of food available for small fish, and so on. Alternatively, a pollutant may cause an overall increase in total phytoplankton (e.g. through eutrophication) but bring about a decrease in zooplankton levels by allowing undesirable algal species to dominate at the expense of species that serve as food for the zooplankton. In this paper we have used mathematical relationships like those described above to generate a series of 'hysteresis relationships

charting the response of each **trophic** level **in** a hypothetical three-level **aquatic** food chain to the pollution and subsequent clean-up of the ecosystem.

We have also assumed, in making our calculations, that the onset of pollution and its clean-up are instantaneous. **This is** perhaps appropriate for longer-lived organisms such **as** fish, but has some **inappropriate** features for algae, which turnover rapidly and thus may respond to intermediate as well **as** initial and final levels of the pollutant. If it proves important to do **so**, a gradual change in pollution may be modeled in future work, but for our initial analysis the step-function approach is more enlightening and expedient.

Biotic Hysteresis: Theoretical Concept

The ecological hysteresis response will resemble the physical hysteresis effect observed in the magnetization of a **ferromagnet**. When a magnet is placed next to an unmagnetized bar of iron, the latter becomes magnetized. When the first magnet **is** taken away, the iron bar loses its magnetic properties much more slowly than it gained them. Similarly, as the level of pollution **in** an aquatic ecosystem **is** decreased, the biological response to the decrease does not trace out in reverse the path it followed in response to the initial pollution of the **system**. Nevertheless, ideally, the system, returns to **its** starting point. For the purposes of this paper we define 'ideal' biotic hysteresis to occur when a population of organisms perturbed by pollution returns to its initial population level within a period of time short enough to be relevant to policy decisions. This time period might be 10 to 20 years. In an ecosystem with several **trophic** levels (**phytoplankton**, large **zooplankton** and **small** fish, and large **fish**, i.e. producers, grazers, and large carnivores) and a single type of pollutant (such as sewage) a series of response-and-recovery curves such as **those** shown **in** Figure 4 would be

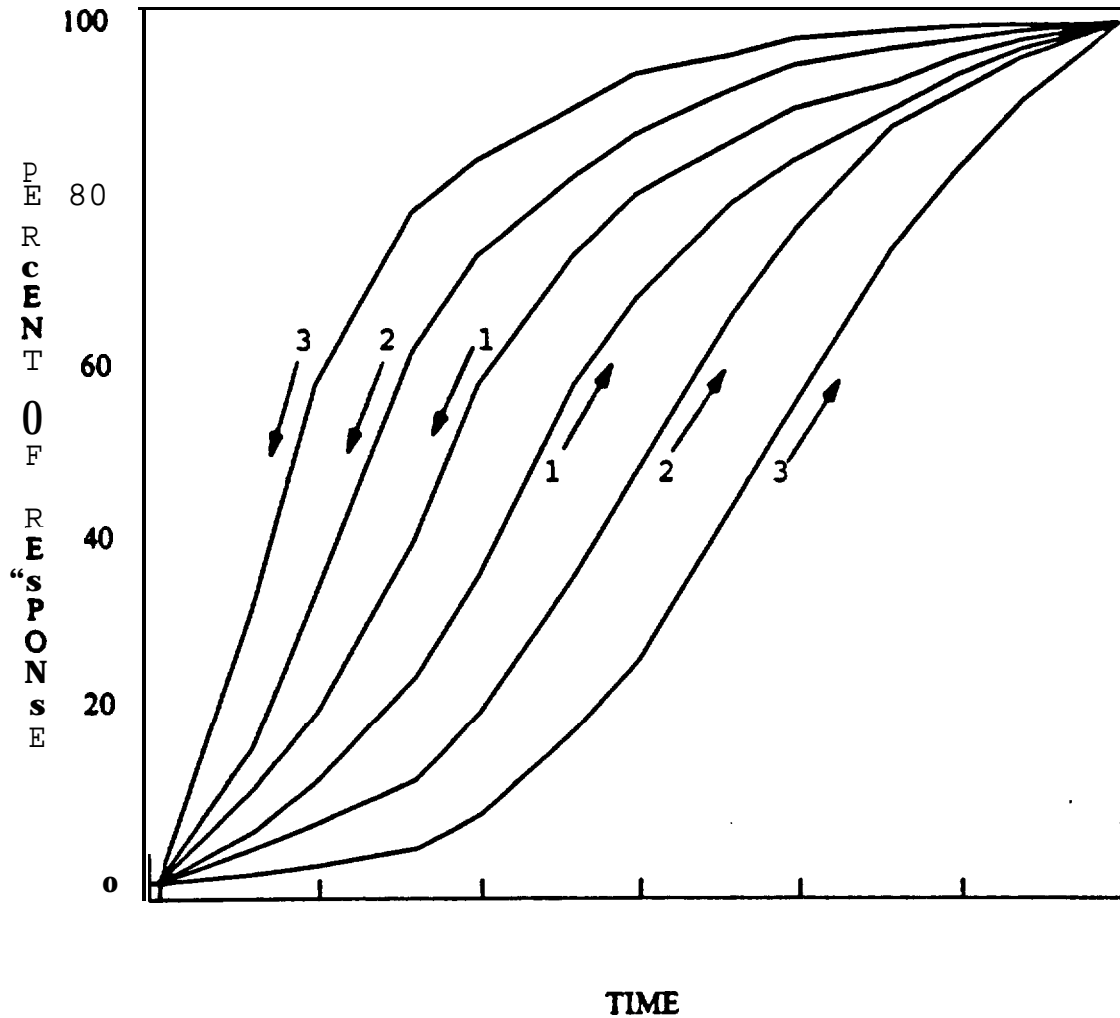


Figure 4. A theoretical distribution of ideal hysteresis curves for an aquatic ecosystem with three **trophic** levels. Curves marked "1" represent the time-path of the response of a population in a lower **trophic** level (e.g. **phytoplankton**) to a pollutant stress and the path of recovery once the stress has been removed. 'Response' paths are marked with left-to-right arrows, while 'recovery' paths are indicated by right-to-left arrows. Curves marked "2" and "3" represent time-paths for middle (e.g. **zooplankton**) and **higher** (e.g. **fish**) **trophic** levels, respectively. Note that populations in higher **trophic levels** exhibit greater lags in both response and recovery than those in lower **trophic** levels.

expected. Even the rapidly **growing phytoplankton** (generation time 1-10 days) can **exhibit** an Ideal hysteresis response **to** the pollutant. For higher **trophic** levels (**copepod** zooplankton and fish), which respond to the altered **phytoplankton** population, there will be a delay in the initiation **of** the exponential section of the curve in Figure 4 **in** rough proportion to the generation time. A delay must occur because complex organisms are incapable of rapidly increasing their number (that **is**, they have a slow numerical response) on a time scale of days. It **will** thus take at least the **adult-to-birth-to-juvenile** period before **copepods** or small fish can show any numerical response to the perturbation, and this response period will be slightly shorter than **the** complete generation time. This lag in response has the interesting consequence that the last half of the change **will** occur more rapidly for high than for low **trophic** levels. Such rapid changes would be of serious concern to resource managers since the response of pollution-control agencies may be too late to protect the resource before the numbers of important organisms are seriously depleted. These **rapid** changes do in fact seem to happen (see Goldman and Home, 1983). Concern about such changes **is** compounded by the fact that **it** is difficult to measure changes **in** biomass stocks at higher **trophic** levels, such as fish. The statistical resolution for fish stock estimation is usually so poor that the majority of a **fish** population can be lost before biologists can detect the change with any certainty.

The **ideal** hysteresis effect is characterized by a cyclic (on a 10-20 year time scale) **non-retracable** path when the response of organisms⁴ to pollution

'In figures 4 and 5 the response of each **trophic** level is normalized **so** that the 'percent **response**' at each time point is given as a percentage of the difference between the population of the organism before the system was perturbed and the population at the point where the pollutant **is** removed. Thus these curves show increasingly lagged responses and recoveries from pollutant stresses, but do not reflect the relative magnitudes of the responses to pollution that might be shown by the different **trophic** levels.

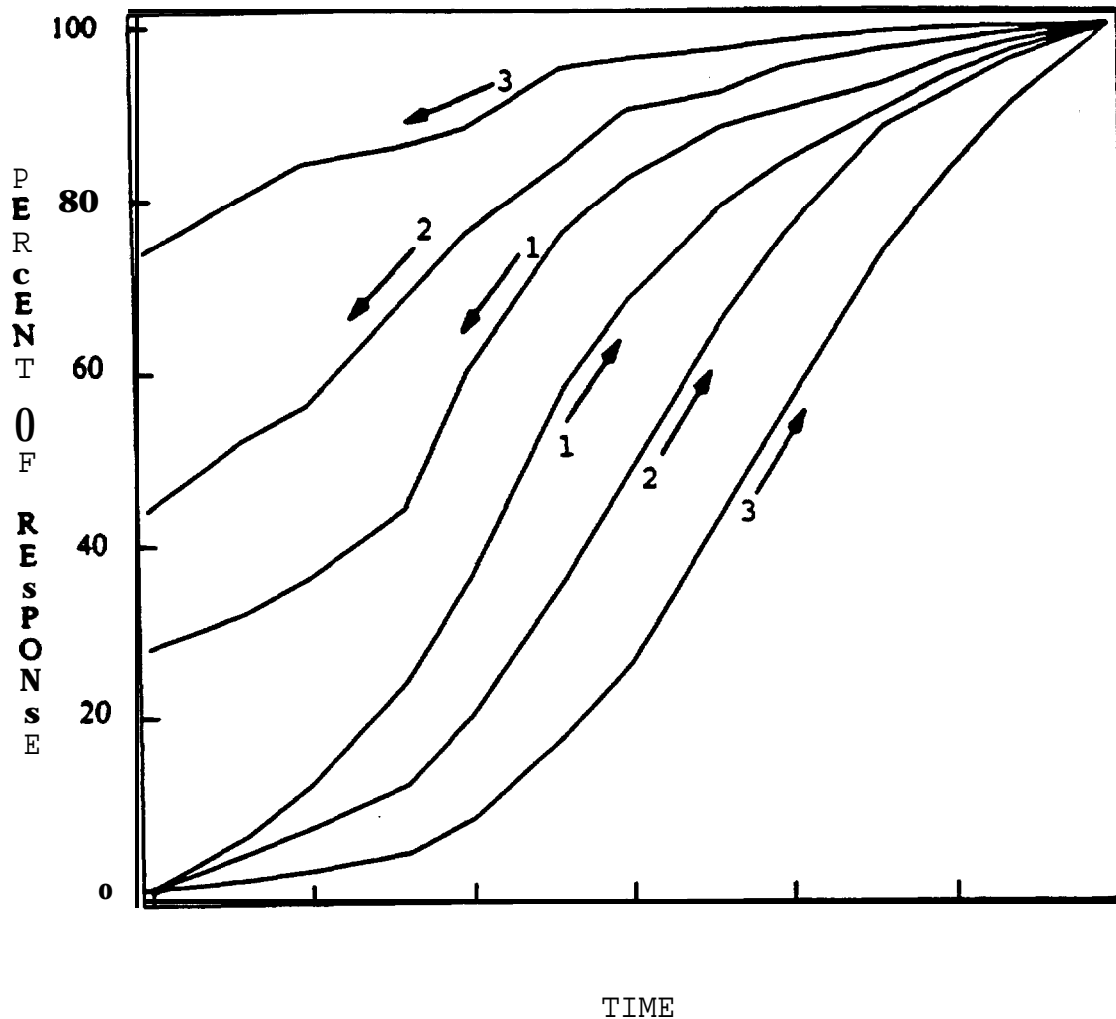


Figure 5. A theoretical distribution of non-ideal hysteresis curves for an aquatic ecosystem with three trophic levels. Curves marked "1" represent the time-path of the response of a population in a lower trophic level (e.g. phytoplankton) to a pollutant stress and the path of recovery once the stress has been removed. 'Response' paths are marked with left-to-right arrows, while 'recovery' paths are indicated by right-to-left arrows. Curves marked "2" and "3" represent time-paths for middle (e.g. zooplankton) and higher (e.g. fish) trophic levels, respectively. In this case, unlike the ideal theoretical case presented in figure 4, the populations do not recover completely within a recovery period of the same duration as the original stress.

is plotted against **time** for a regime in which a pollutant **is** added (left-to-right paths **in** figures 4 and 5) then removed (right-to-left paths). A damped hysteresis effect **is** also possible. This effect, **which** we have termed 'non-ideal' biotic hysteresis, **is** characterized by **non-retracable** and non-cyclic behavior (as shown **in** figure 5), is also possible. A possible explanation of such behavior for a specific food chain (rather than a food chain of generalized **trophic** levels) is the following. If a species of plant or animal remains at depressed levels (e.g. as a result of a pollutant-related stress) for long periods there is in effect a vacant niche that can be occupied by a pollution-tolerant species or even another species that has no **direct** effect **on** the fish of concern (Christie, 1974). Generally the replacement species are less highly regarded by sports and/or commercial fisheries groups and are an economically inferior substitute for the original species. **Thus** if the return leg of the hysteresis curve **is** very flat after cessation of pollution, organisms at the valuable higher **trophic** level may be subject to 'species replacement or "**competitive displacement**" and never return to their original dominant position.

Methods and Initial Results from the Hysteresis **Trophic-Link Model (HTLM)**

Our objective **in** this modeling effort was to test a simple approach for describing mathematically the hysteresis phenomenon discussed above. The purpose of the model described here is solely to illustrate how a generalized ecological phenomenon of interest (hysteresis) can be demonstrated using mathematical relationships containing easily identifiable and understandable parameters. In this approach a food chain with three **trophic levels-- phytoplankton, zooplankton, and small fish--was assumed.** The rate of change of the populations **in** the first two **trophic** levels were described by differential equations (1) and (2) above, and the rate of change of the

population in the third trophic level was described by

$$(3) \quad \frac{dZ}{dt} = E_{yz}B_{yz}YZ - b_zZ, \text{ where}$$

Y , Z , and b_z are as previously described,

E_{yz} = that fraction of biomass in the Y th trophic level that becomes incorporated in the Z th level, and

b_z = a rate constant describing the loss of small fish due to old-age death and other donor-controlled mechanisms.

The constants in the three equations were obtained by assuming a value of 0.1 for r_x and E_{yz} , and a value of $2 \times X^*$ for K_x . The values for X^* , Y^* , and Z^* , the steady-state biomass populations for the three trophic levels (that is, the relative amounts of per-unit-area biomass for which dX/dt , dY/dt , and $dZ/dt = 0$) were taken to be 50, 10, and 1, respectively. Generation times for the three trophic levels (T_x , T_y , and T_z) were taken to be 3, 20, and 360 days, respectively. The following relationships were used to derive the values of r_x , B_{xy} , and B_{yz} :

$$r_x = T_x^{-1},$$

$$E_{xy}B_{xy}X^* = T_y^{-1},$$

$$E_{yz}B_{yz}Y^* = T_z^{-1}.$$

values for b_x , b_y and b_z were derived from the steady-state forms of equations (1) through (3).

Equations (1) through (3) were incorporated into a fortran computer program, which was used to approximate the time path of populations X , Y , and Z in response to a perturbation in r_x , the phytoplankton. The program calls the NAG (Numerical Algorithm Group, 1984) subroutine **D02EBF**, which integrates systems of differential equations using a variable-order, variable-step Gear method and returns solutions to the system ($X(t)$, $Y(t)$, $Z(t)$) at specified

time points. Details of the model and a listing of the integration program are given in the appendix to this paper.

We should note that an analytical approximation to the solution of equations (1) - (3) can be obtained by adding a fourth equation, namely

$$(4) \quad \frac{dr_x}{dt} = 0$$

to the system, deriving a 4 x 4 "community matrix" using procedures described by May (1973) and Harte (1985), and using that matrix to explore the effects of perturbations to the system. A four-level food-chain model was also developed. This model, which adds a larger piscivorous fish to the three-tiered food chain, uses equations (1) - (3), above, with the term $-B_{zf}ZF$ added to equation (3). A fourth equation,

$$(5) \quad \frac{dF}{dt} = E_{zf}B_{zf}ZF - b_f F.$$

is added to model the behavior of the population of larger fish (F). In this system the steady-state biomass ratios in the four trophic levels were taken to be 500 : 100 : 10 : 1 ($X^* : Y^* : Z^* : F^*$), the generation time for the larger fish (T_f) was taken to be 1080 days, E_{zf} was taken to be 0.1, and $E_{zf}B_{zf}ZF$ was defined to equal T_f^{-1} . This four-level system was solved as above. Details of the model and a listing of the computer program used to solve it are given in the appendix.

Results

The time paths traced by the three "populations" (here taken to mean biomass present in each trophic level per unit area of water) following a -2% reduction in r_x are shown in figure 6. The population of phytoplankton drops rapidly in response to the reduction in its growth rate, reaching a local

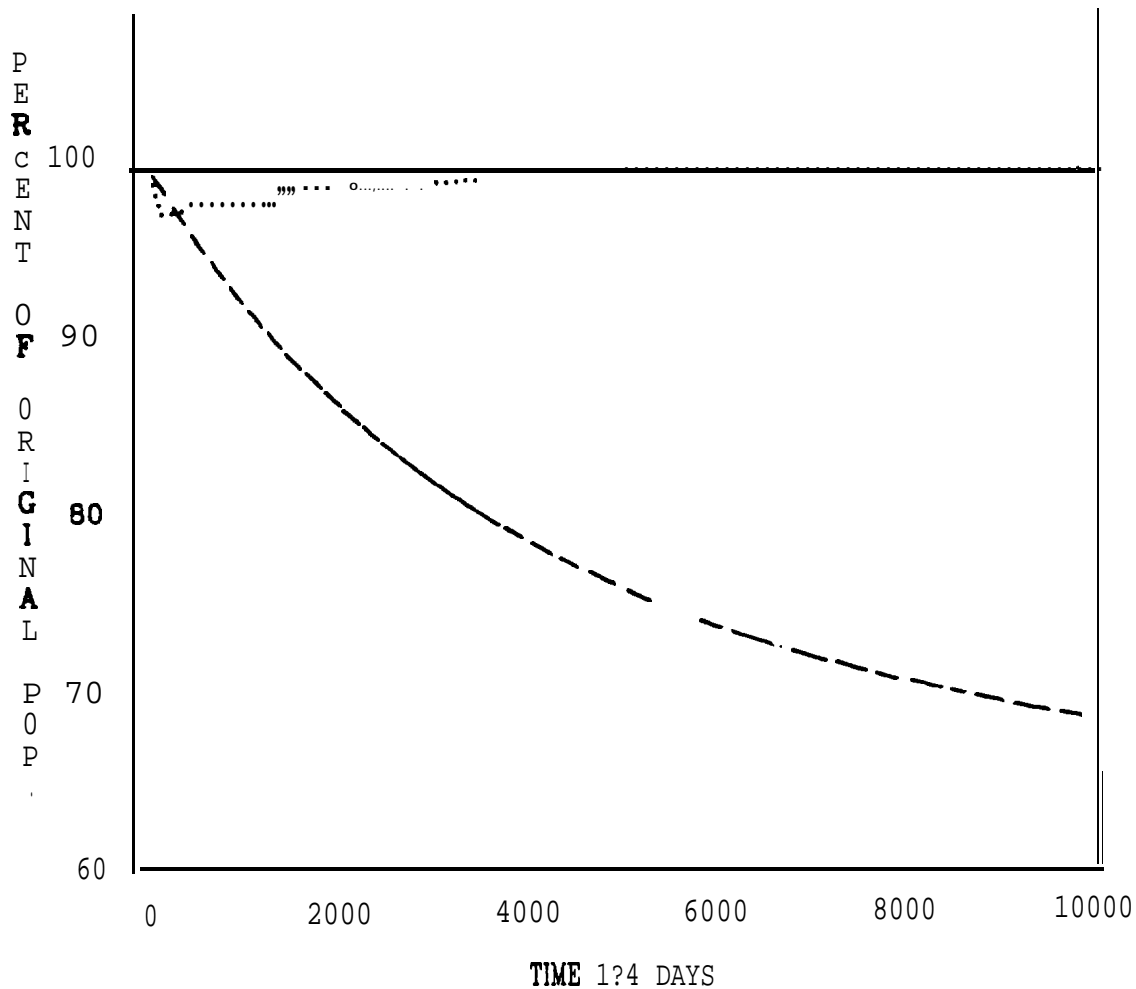


Figure 6. Calculated time paths for the response of the populations (measured in biomass per unit area, initial biomass ratios: **50 phytoplankton: 10 zooplankton : 1 small fish**) in a three-tiered aquatic food chain to a **-2%** change in the growth rate of **phytoplankton**. Solid, dotted, and (partially) dashed lines give the paths for **phytoplankton**, **zooplankton**, and **small fish**, respectively. Note that the lower **trophic** levels respond more quickly to the stress than higher **trophic** levels, but the ultimate effect on higher **trophic** levels is greater in magnitude.

minimum **in 20 days** (not visible in **figure 6** due to the length of the time scale). Thereafter the population **rises** quickly, then **falls** slowly **in** response to the changes **in** the population of **its** predator (**zooplankton**). By the time 10,000 days (about 30 years) have elapsed, the **phytoplankton** population reaches a steady-state value equal to **99%** of **its** original level. The population of **zooplankton** drops more slowly, but over a longer period. For this second **trophic** level the maximum deviation from the original population, **-3.5%**, occurs after 150 days. From there the **zooplankton** population rises to a level about 1% above that originally present. The population of small fish declines more slowly than those of either of the lower **trophic** levels, but in time **exhibits** a greater response, reaching a new steady-state population **70%** as large as the original group. Note that the deviations in the zooplankton and fish populations are out of phase with each other. This makes sense ecologically **as well as** mathematically: **as** fish populations decline, grazing pressure on zooplankton is decreased, allowing that population to expand. Perhaps the most important result shown in figure 6, however, is that a small (**-1%**) perturbation in the **phytoplankton** growth rate produces a large (**-30%**) change in the population at the highest **trophic** level.

Figures 7-10 present time paths for the three populations in which a **-2%** perturbation **in r_x is applied** at time **zero**, then removed at **300, 500, 2000,** and **10,000 days**, respectively. Paths for which arrows point left-to-right chart the response **of** the three populations to the original perturbation, **while** paths with right-left arrows chart the return paths for time periods of the same duration as the original perturbation. Thus **in** figure 7, for example, the solid curve labeled with a right-pointing arrow **charts** the response of the **phytoplankton** population to a perturbation applied for **300** days, while the solid path labeled with a left-pointing arrow charts the level

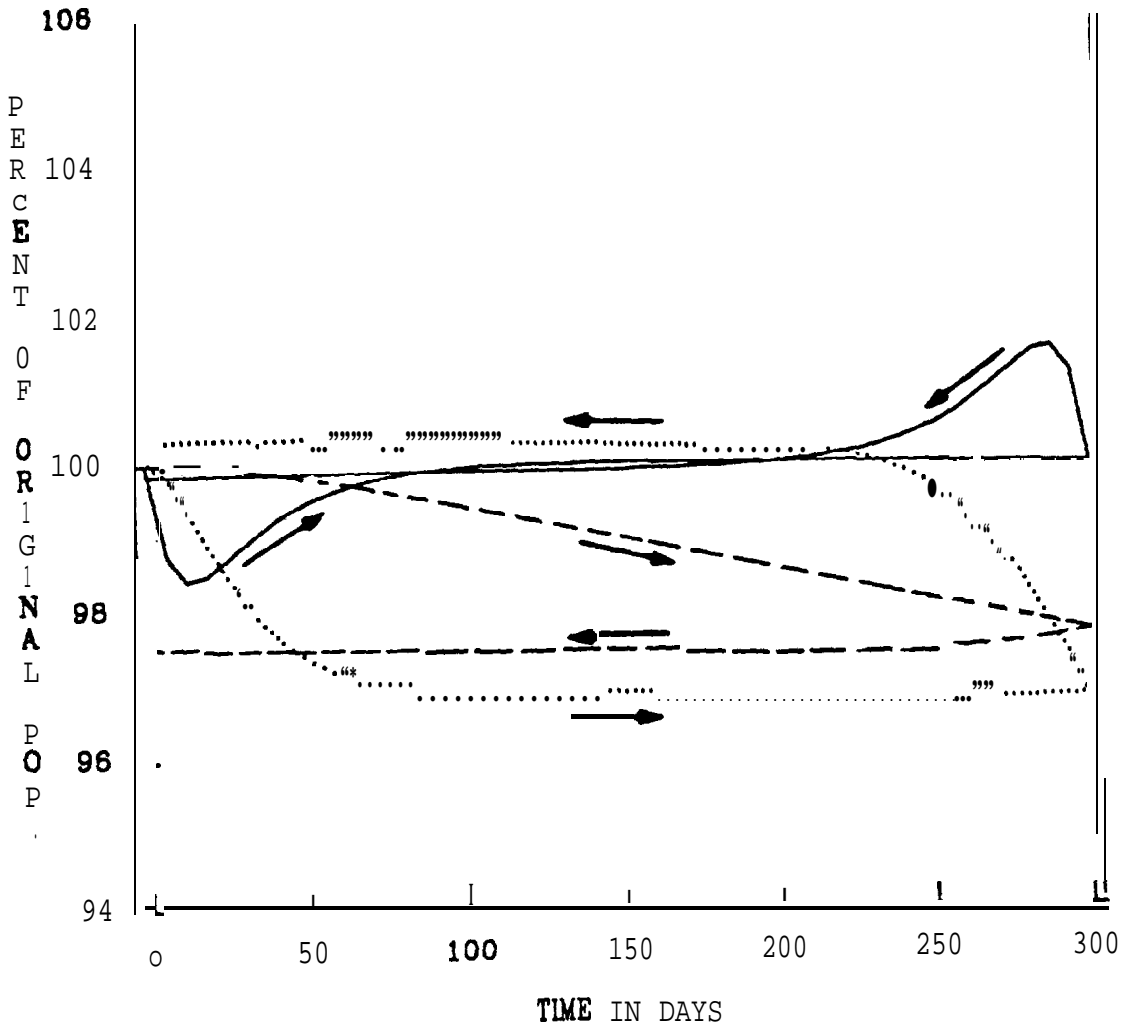


Figure 7 Calculated time paths for the response and recovery of the populations (measured in biomass Per unit area, initial biomass ratios: 50 phytoplankton: 10 zooplankton : 1 small fish) in a three-tiered aquatic food chain when a -2% perturbation in the phytoplankton growth rate is applied at time zero, then removed after 300 days. "Response" paths are indicated by right-pointing arrows, and "recovery" paths are marked with left-pointing arrows. Solid, dotted, and (partially) dashed lines give the paths for phytoplankton, zooplankton, and small fish, respectively. Note that the population of small fish continues to decline even after the perturbation is removed, and fails to return to its original position after 300 days of recovery.

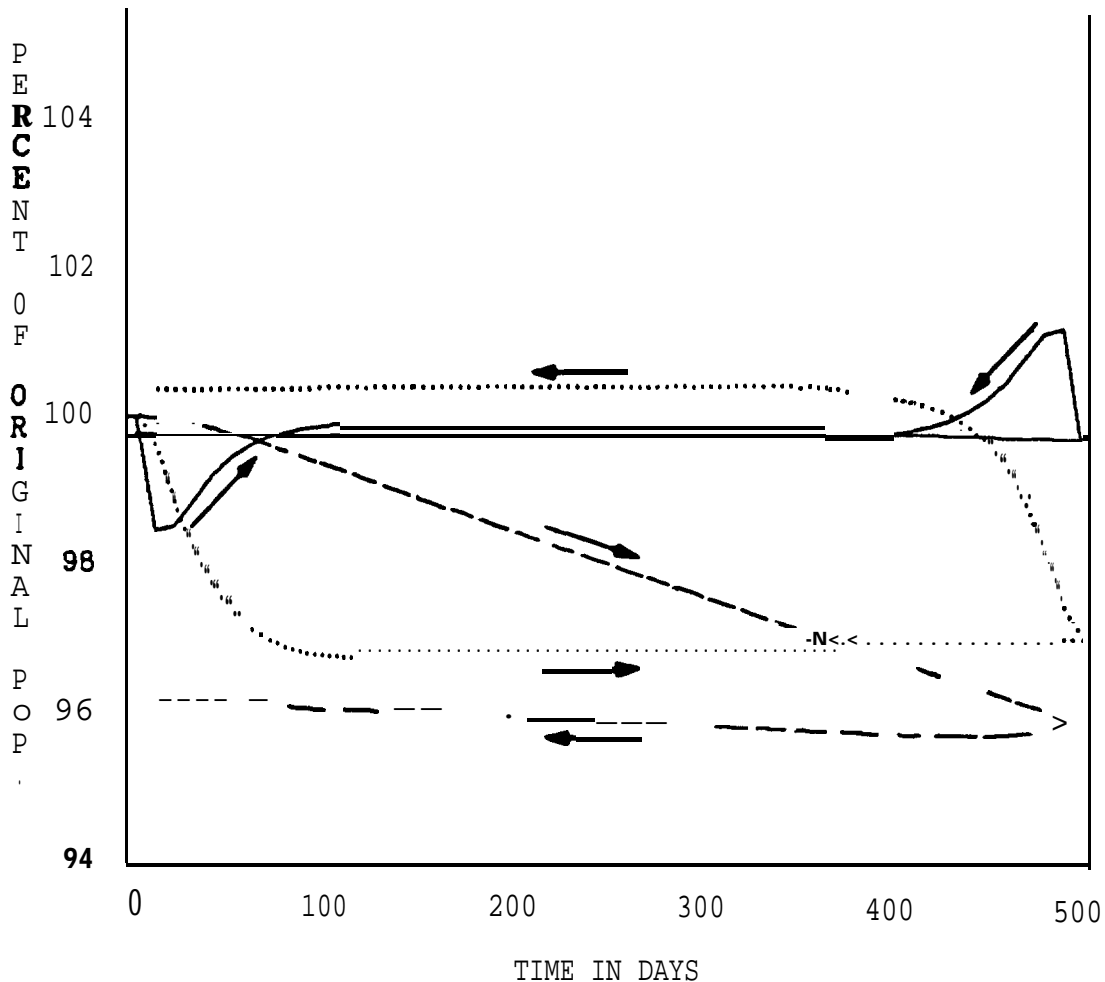


Figure 8 Calculated time paths for the response and recovery of the populations (measured *in* biomass per unit area, initial biomass ratios: 50 phytoplankton: 10 zooplankton : 1 small fish) in a three-tiered aquatic food chain when a -2% perturbation in the phytoplankton growth rate is applied at time zero, then removed after 500 days. 'Response' paths are indicated by right-pointing arrows, and 'recovery' paths are marked with left-pointing arrows. Solid, dotted, and (partially) dashed lines give the paths for phytoplankton, zooplankton, and small fish, respectively. Note that the population of small fish shows a lag of approximately 50 days before beginning its recovery.

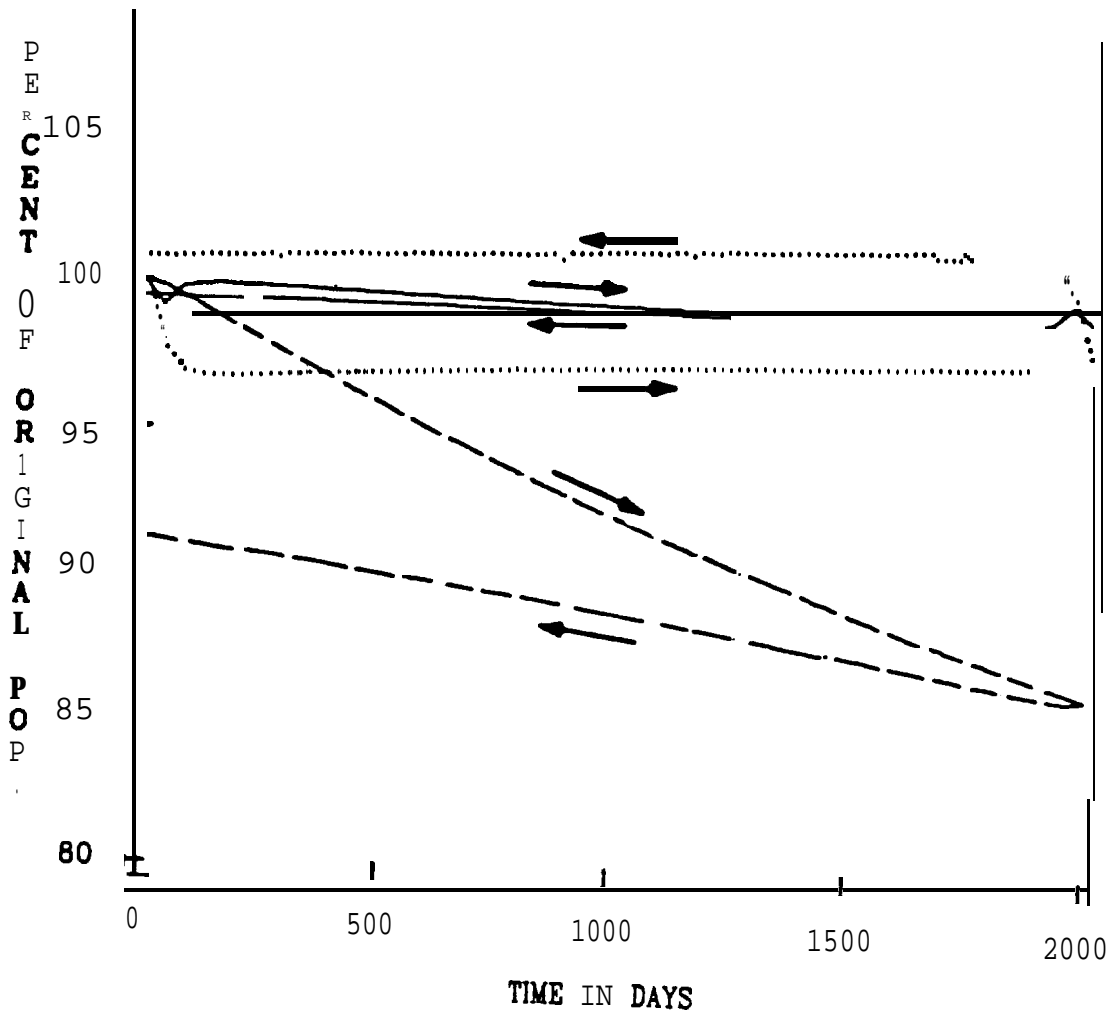


Figure 9 Calculated time paths for the *response* and recovery of the populations (measured in biomass per unit area, initial biomass ratios: 50 phytoplankton: 10 zooplankton : 1 small fish) in a three-tiered aquatic food chain when a -2S perturbation in the **phytoplankton** growth rate is applied at time zero, then removed after 2000 days. 'Response' paths are indicated by right-pointing arrows, and "recovery" paths are marked with left-pointing arrows. Solid, dotted, and (partially) dashed lines give the paths for **phytoplankton**, **zooplankton**, and **small fish**, respectively. Note that the population of small fish fails to return to its initial level after 2000 days of recovery.

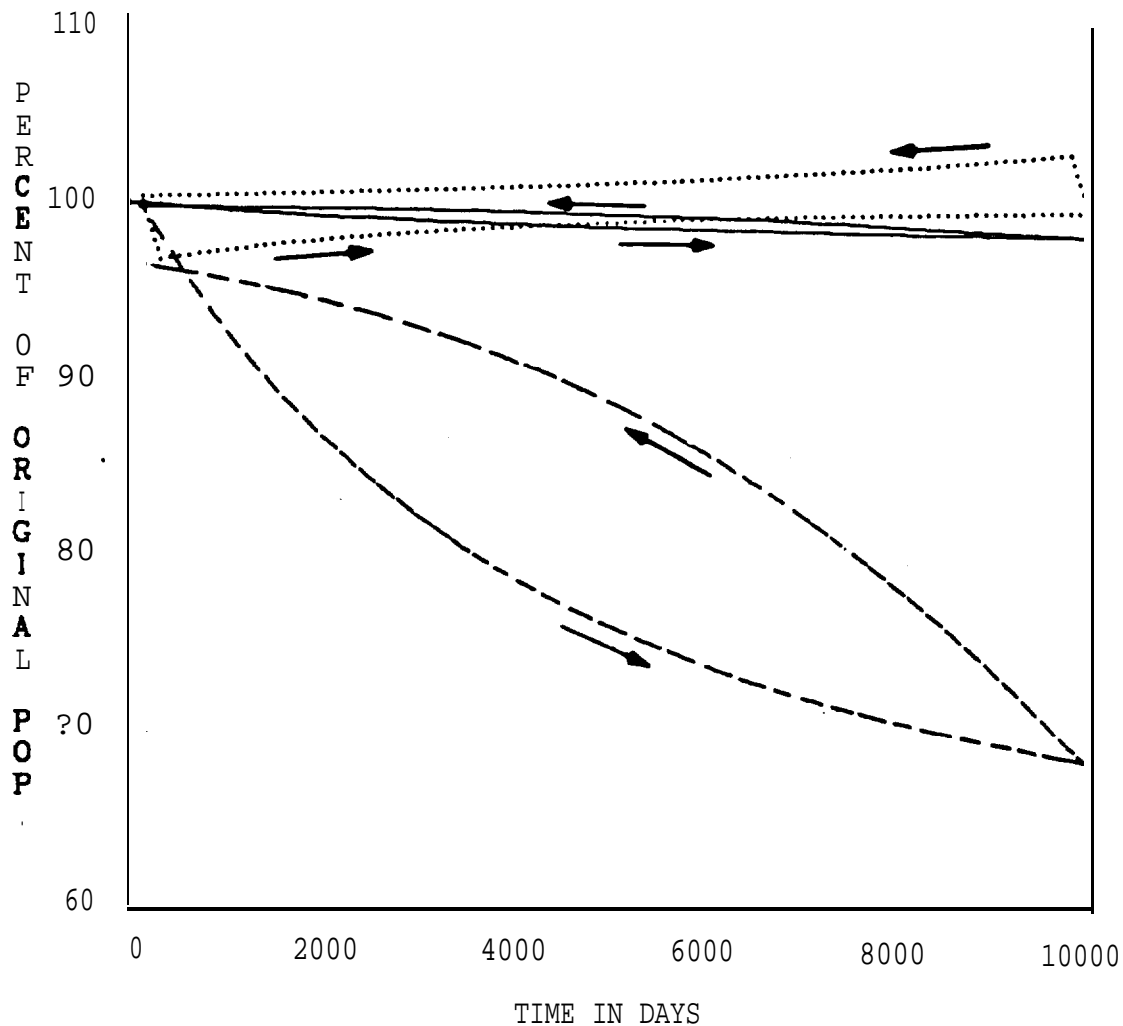


Figure 10 Calculated time paths for the response and recovery of the populations (measured in biomass per unit area, initial biomass ratios: 50 phytoplankton: 10 zooplankton : 1 small fish) in a three-tiered aquatic food chain when a -2S perturbation in the phytoplankton growth rate is applied at time zero, then removed after 10,000 days. 'Response' paths are indicated by right-pointing arrows, and 'recovery' paths are marked with left-pointing arrows. Solid, dotted, and (partially) dashed lines give the paths for phytoplankton, zooplankton, and small fish, respectively. Note that the population of small fish falls to return to its initial level even after 10,000 days of recovery.

of the **phytoplankton** population after the perturbation **is removed**. For the return paths time runs right-to-lefts thus the points on the return paths directly above "50" on the time axis are actually 250 days from the point where the perturbation was removed. The presentation of the hysteresis **curves** in figures 7-10 are different from those **in** figures 4 and 5 **in** that they are **not** normalized **to** the response of each population to the perturbation, rather they indicate the percentage change **in** each population. **This** allows the relative magnitudes of the population changes **in** the different **trophic** levels as well as the shapes of the hysteresis curves to be compared.

Figures 7-10 present a series of hysteresis curves **in** which time paths for the fish populations show a progression from non-ideal- toward **ideal-** hysteresis behavior, as those terms are defined above. For each time interval the **phytoplankton** population can be seen, after perturbation of the system, to decline rapidly to **just above 98% of its original level, remaining** near that value for the duration of the perturbation. When the stress is removed, the **phytoplankton** population quickly increases to **2% over its pre-** perturbation level, then declines to its original level and remains relatively stable thereafter. In each of figures 7-10 the zooplankton population decreases rapidly following, perturbation, then drifts slowly higher as fish populations decline. **When** the perturbation is removed zooplankton quickly increase, due to the increased availability of **phytoplankton**, then decline slowly to near their original level as fish populations increase. The population of fish **shows a slow and steady decline over a 300-day** perturbation. The decline continues for about 150 days after **the** perturbation **is removed**. In figure **8**, the fish population again declines throughout the perturbation period and into the return period, but starts to recover approximately 50 days after the perturbation **is removed**. Figure 9 shows even less lag before the fish population starts to recover. Figures **7-**

